Optimal quantum parameter estimation in a pulsed quantum optomechanical system

Qiang Zheng,[1,2] Yao Yao,[1,3] and Yong Li[1,4]

[1]*Quantum Physics and Quantum Information Division, Beijing Computational Science Research Center, Beijing 100084, China*
[2]*School of Mathematics and Computer Science, Guizhou Normal University, Guiyang, Guizhou 550001, China*
[3]*Microsystems and Terahertz Research Center, China Academy of Engineering Physics, Chengdu, Sichuan 610200, China*
[4]*Synergetic Innovation Center of Quantum Information and Quantum Physics, University of Science and Technology of China, Hefei, Anhui 230026, China*

(Received 29 July 2015; published 25 January 2016)

We propose that a pulsed quantum optomechanical system can be applied to the problem of quantum parameter estimation, which targets yielding a higher precision of parameter estimation utilizing quantum resources than using classical methods. Concentrating mainly on the quantum Fisher information with respect to the mechanical frequency, we find that the corresponding precision of parameter estimation for the mechanical frequency can be enhanced by applying applicable optical resonant pulsed driving to the cavity of the optomechanical system. Further investigation shows that the mechanical squeezing resulting from the optical pulsed driving is the quantum resource used in optimal quantum estimation of the frequency.

DOI: 10.1103/PhysRevA.93.013848

I. INTRODUCTION

Quantum metrology [1] has been an active research field in recent years. According to the quantum Cramér-Rao inequality, the quantum Fisher information (QFI) plays a key role in this subject [2–6], which bounds the minimal variance of the unbiased estimator. The QFI gives the quantum limit on the accuracy of the estimated parameter with any positive-operator-valued measurement. One of the central ideas of quantum metrology is to beat the shot-noise limit and approach the Heisenberg limit by virtue of quantum resource, such as quantum entanglement or squeezing. There have been many studies on the precision of parameter estimation with a sub-shot-noise limit in different physical systems, such as optical interferometers [7–9], Bose-Einstein condensates [10], atomic interferometers [11], and solid-state systems (e.g., nitrogen-vacancy centers) [12,13]. To the best of our knowledge, only a few papers [14–16] have been devoted to investigating the quantum metrology in the newly developed novel quantum optomechanical device.

With the rapid advance of technology, quantum cavity optomechanics [17–19], in which the mechanical resonator is coupled to the optical field by radiation pressure or photothermal force, has excited a burst of interest [20] for the following two reasons: On one hand, the cavity optomechanical system provides a new platform for investigation of the fundamental questions on the quantum behavior of macroscopic systems [21] and even the quantum-to-classical transition [22,23]; on the other hand, it brings a novel quantum device for applications in ultrahigh-precision measurement [24–28], gravitation-wave detection [29], quantum information processing [30], and quantum illumination [31]. Much interesting research in cavity optomechanical systems, such as optomechanically induced transparency [32,33], ground-state cooling of the mechanical resonator [34–38], optomechanical entanglement [39,40], and optimal state estimation [41], has been reported. These studies mainly rely on the enhanced coupling strength between the phonic and the photic fields by strongly pumping the optical cavity with a continuous-wave (CW) laser.

Differently from the above case of CW laser driving, so-called pulsed quantum optomechanics [42], is also realized by driving the optical cavity with (very) short optical pulses. Originally, this strategy was proposed in systems of qubits [43], and recently it was extended to atomic ensembles [44] and levitated microspheres trapped in an optical cavity [45]. Compared with the CW-laser-driving case, the benefit of the pulsed scheme is that it does not require the existence of a stable steady state for the optomechanical system. The pulsed interaction has also displayed its superiority in preparing and reconstructing the quantum state of the mechanical resonator [46,47], enhancing optomechaical entanglement [48,49] and EPR steering [50], and cooling the mechanical mode [51,52].

Inspired by the experimental progress in pulsed quantum optomechanical systems [42,49,51], it is a natural idea to investigate the high precision of parameter estimation by applying optical pulsed driving to the cavity of the optomechanical system. Here we investigate a special pulsed optomechanical system, where the coupling between the mechanical mode and the cavity field is quadratical to the mechanical motion and the cavity field is resonantly driven with external optical pulses. We mainly focus on the QFI with respect to the mechanical frequency, which is equivalent to estimating the mass of the mechanical resonator and could be used for mass precision detection. With the Cramér-Rao inequality, a larger QFI implies that the mechanical frequency can be estimated with a higher precision. We show that the QFI can be greatly enhanced when the period of the driving pulse matches that of the mechanical motion. We also show that the mechanical squeezing resulting from the resonant driving pulses is the quantum resource strengthening the QFI.

This paper is organized as follows. The pulsed quantum optomechanical model is discussed in Sec. II. We investigate in Sec. III the QFI of the pulsed quantum optomechanical system with respect to the mechanical frequency. Then we demonstrate that quantum squeezing is the resource used in optimal quantum estimation. Finally, a summary is given in Sec. IV. The basic properties of the QFI, especially the QFI of a single-mode Gaussian state, are reviewed in the Appendix.

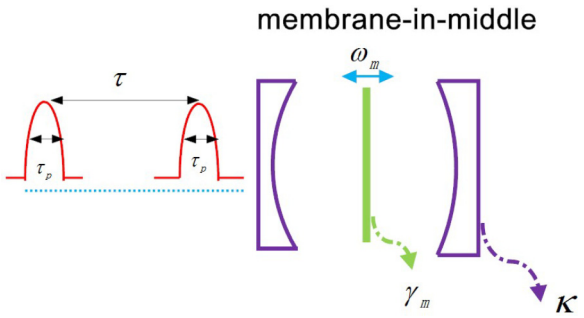

FIG. 1. Schematic the membrane-in-the-middle cavity optomechanical setup considered in this paper. The coupling between the cavity field (with decay rate κ) and the mechanical resonator (with resonance frequency ω_m and damping rate γ_m) is quadratical to the mechanical motion, and the driving field is composed of a series of periodic pulses. The duration of one pulse is τ_p, and two consecutive pulses have the time interval τ.

II. PULSED QUANTUM OPTOMECHANICS

Optomechanical systems have been implemented in many physical systems, such as suspended mirrors in Fabry-Pérot resonators [53], toroidal whispering gallery mode resonators [54], trapped levitating nanoparticles [55], and ultracold atomic clouds in cavities [56]. Here we focus on a membrane-in-the-middle cavity optomechanical setup [57], which has been used for quantum nondemolition measurement of the phonon number state [58], cooling of the mechanical resonator [59], and investigation of Landau-Zener-Stückelberg dynamics [60]. Linear and quadratical optomechanical couplings between the cavity mode and the mechanical resonator can exist in this membrane-in-the-middle optomechanical system. Very recently, optomechanical quadratical coupling was also achieved in a crystal optomechanical system [61], except for the membrane-in-the-middle setup.

The membrane-in-the-middle quadratical coupling setup under consideration is shown in Fig. 1 and the corresponding Hamiltonian is expressed as [62]

$$H = \frac{\hbar\omega_m}{2}(\hat{p}^2+\hat{q}^2) + \hbar\omega_c\hat{a}^\dagger\hat{a} + \hbar g_2\hat{a}^\dagger\hat{a}\hat{q}^2 + i\hbar[E_0(t)e^{-i\omega_d t}\hat{a}^\dagger - \text{H.c.}]. \quad (1)$$

Here ω_m is the frequency of the mechanical resonator, $\hat{p}$ and $\hat{q}$ are the dimensionless momentum and position operators satisfying the relationship $[\hat{q},\hat{p}] = i$, $\hat{a}$ is the annihilation operator of the cavity mode with resonance frequency ω_c and decay rate κ, and g_2 is the quadratic optomechanical coupling strength. Finally, $E_0(t) = \sqrt{2P_0(t)\kappa/(\hbar\omega_c)}$, with $P_0(t)$ the optical input power. We further assume that the cavity is driven resonantly with $\omega_d = \omega_c$.

For the mechanical resonator, by linearizing the optomechanical coupling, the corresponding quantum Heisenberg-Langevin equation is obtained as

$$\frac{d}{dt}\hat{q} = \omega_m\hat{p}, \qquad \frac{d}{dt}\hat{p} = -\widetilde{\omega}_m(t)\hat{q} - \gamma_m\hat{p} + \xi, \quad (2)$$

where $\widetilde{\omega}_m(t) = \omega_m + A(t)$, with $A(t) = 2g_2 n_a(t)$ and $n_a(t) = \langle\hat{a}^\dagger\hat{a}\rangle$. Here γ_m is the mechanical damping rate, and ξ denotes the Brownian noise with null mean and correlation function satisfying $\langle\xi(t)\xi(t')\rangle = 2n_{\text{th}}\gamma_m\delta(t-t')$ in the high-temperature limit $k_BT \gg \hbar\omega_m$. Here k_B is the Boltzmann constant, T is the temperature of the mechanical resonator, and $n_{\text{th}} = [e^{\hbar\omega_m/(k_BT)} - 1]^{-1} \approx k_BT/(\hbar\omega_m)$ is the mean thermal phonon number.

From Eqs. (2), the dynamics of the second-order moments of the mechanical system

$$\vec{v}(t) \equiv (\langle\hat{q}^2\rangle, \langle\hat{p}\hat{q}+\hat{q}\hat{p}\rangle/2, \langle\hat{p}^2\rangle)^{\text{T}} \quad (3)$$

can be fully described by the equations

$$\frac{d}{dt}\vec{v}(t) = \mathbf{U}_A\vec{v}(t) + \vec{N} \quad (4)$$

for an initial Gaussian state of the mechanical resonator (such as the thermal equilibrium state with mean phonon number n_{th}). Here the superscript T represents the transposition. Also,

$$\mathbf{U}_A = \begin{pmatrix} 0 & 2\omega_m & 0 \\ -\widetilde{\omega}_m & -\gamma_m & \omega_m \\ 0 & -2\widetilde{\omega}_m & -2\gamma_m \end{pmatrix}, \quad (5)$$

and $\vec{N} = [0,0,(2n_{\text{th}}+1)\gamma_m]^{\text{T}}$.

The solution of Eq. (4) is formally expressed as

$$\vec{v}(t) = e^{\mathbf{U}_A t}\vec{v}(0) + \int_0^t e^{\mathbf{U}_A(t-t')}\vec{N}\,dt' = \mathbf{M}_A(t)\vec{v}(0) + \vec{v}_{\text{inh}}. \quad (6)$$

Here $\mathbf{M}_A(t) = e^{\mathbf{U}_A t}$ and $\vec{v}_{\text{inh}} = \mathbf{U}_A^{-1}[\mathbf{I}_3 - \mathbf{M}_A(t)]\vec{N}$, with $\mathbf{I}_3$ being a 3×3 unitary matrix.

Now we study the case where the driving field is periodic Gaussian pulses with duration τ_p and period τ; i.e. $P(t) = P_0\sum_n \exp[-(t-n\tau)^2/\tau_p^2]$. Here we keep the condition $1/\tau_p < c/2L$ (L is the cavity length), which means that the optical driving pulses will not excite the near-cavity modes except the desired one, and thus the cavity field can always be considered a single-mode one. To retain the quadratic coupling during the pulsed driving, the membrane should be locked at a cavity node. Accordingly, the effective frequency of the mechanical resonator is periodically modulated in time via the optical driving pulses. An alternative scheme for achieving periodic modulation of the effective frequency of the mechanical resonator is given in Ref. [63] with a two-tone drive.

Moreover, we assume that the system works in the following parameter regimes: (i) $1/\tau \ll \kappa$, (ii) $1/\tau_p \ll \kappa$, and (iii) $\tau_p \ll 1/\omega_m$. Condition (i) implies that the cavity is rapidly excited by one pulse and damps to the vacuum state before the next pulse arrives [46]. And condition (ii) means that the bandwidth of the pulses is much smaller than that of the cavity, which guarantees that the pulse enters the cavity spectrally. The last condition, (iii), ensures that the free rotation of the mechanical resonator is frozen in the process of the pulse-mirror interaction. In this case, the intracavity photon number can be approximated as a series of Dirac delta functions $n_a(t) \propto \sum_{n=0}\delta(t-n\tau)$ in the typical evolution time of the mechanical resonator. As a result, the entire dynamics of the optomechanical system is divided into two steps: (i) one kick at time $t = n\tau$, which can

be described by the unitary operator $U_{\rm K} = e^{-i\theta\hat{q}^2}$, with $\theta = g_2 \int_{\Delta t} n_a(t)dt$ being the kick strength (Δt is the integral time domain and is of the order of the typical time for a Gaussian pulse), and thus corresponds to the linear transformation $q \to q$ and $p \to p - 2\theta q$; and (2) the free-evolution lasting time τ between two adjacent kicks, whose corresponding evolution is determined by Eq. (2) with $A(t) = 0$.

Combining these two evolving processes, the equation of motion in a τ circle is given as [46]

$$\overrightarrow{v}((n+1)\tau) = \mathbf{M}_0(\tau)\mathbf{K}\overrightarrow{v}(n\tau) + \overrightarrow{v}_{\rm inh}(\tau), \tag{7}$$

where $\mathbf{M}_0(\tau) \equiv \mathbf{M}_{A=0}(t)|_{t=\tau}$ and

$$\mathbf{K} = \begin{pmatrix} 1 & 0 & 0 \\ -2\theta & 1 & 0 \\ 4\theta^2 & -4\theta & 1 \end{pmatrix}, \tag{8}$$

denoting the effect of the kick on the second-order moments. That is, $\mathbf{K}$ is the representation of $U_{\rm K}$ based on the second-order moments. Making use of Eq. (7), the stroboscopic state of the mechanical resonator at time $t = n\tau$ is obtained as

$$\overrightarrow{v}(n\tau) = (\mathbf{M}_0(\tau)\mathbf{K})^n \overrightarrow{v}(0) + [\mathbf{I}_3 - (\mathbf{M}_0(\tau)\mathbf{K})^n](\mathbf{I}_3 - \mathbf{M}_0(\tau)\mathbf{K})^{-1}\overrightarrow{v}_{\rm inh}(\tau). \tag{9}$$

III. QFI OF PULSED OPTOMECHANICS

After the detailed presentation of the pulsed quantum optomechanical model in the previous section, here we investigate the quantum parameter estimation via the related QFI in this model. We also show that the quantum resource used for parameter estimation is the squeezing produced by pulsed driving.

A. Primary discussion

The parameter to be estimated in this paper is the frequency ω_m of the (harmonic) mechanical resonator. Choosing this parameter is based on the following consideration. With the relation $\omega_m = \sqrt{k_m/M}$ (k_m and M being the spring constant and the mass, respectively), the QFI with respect to M is proportional to that with respect to ω_m, that is,

$$F_{\rm M} = \mu F_{\omega_m}, \tag{10}$$

where $\mu = \frac{k_m}{4M^3}$ is the scaling factor. As a result, the estimation of M, just as done in the mass spectrometer [64], is equivalent to the estimation of ω_m. In principle, the parameters to be estimated in this model can be those other than ω_m (m). Here we concentrate on the case of ω_m via its related QFI, $F \equiv F_{\omega_m}$.

The numerical values of the parameters used in this paper are based on the state-of-the-art experiments reported in Ref. [65]. We choose the cavity decay as $\kappa \simeq 10^2$ GHz and driving pulses with duration $\tau_p = 0.1$ ns. We also set the mechanical frequency $\omega_m = 0.5 \times 10^6$ Hz and the damping rate $\gamma_m = 10^2$ Hz unless otherwise stated. By carefully choosing the mechanical mass, reflectivity, and initial equilibrium position, the kick strength θ is in the range of (0.01,10) for the typical coupling strength g_2.

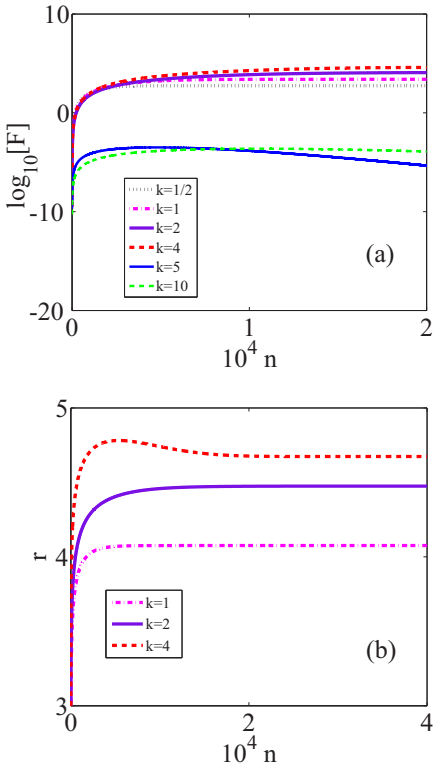

FIG. 2. Variation of (a) the QFI F and (b) the squeezing degree r defined in Eq. (12) in terms of the pulse number n, respectively. Different lines correspond to different values of the parameter $k = T_0/\tau$ (τ being the period of the pulses and $T_0 = 2\pi/\omega_m$). The other parameters are $n_{\rm th} = 100$ and $\theta = 1.0$. The QFI F is in units of Hz^{-2}.

B. Numerical results of the QFI

By substituting Eq. (9) into Eq. (A10), the QFI F can be obtained straightforwardly. Fortunately, the last term in Eq. (A10) vanishes since there is no first-order moment of the mechanical motion. In what follows, we mainly explore F by numerical simulations, as the analytical solution is too cumbersome.

With extensive numerical simulations, we find that the evolution of F in terms of the pulse number n shows two distinct behaviors, as shown in Fig. 2(a). In this figure, the period of pulse τ matches that of the mechanical resonator T_0 ($\equiv 2\pi/\omega_m$) though $\tau = T_0/k$, with k taking the representative values $\{\frac{1}{2},1,2,4,5,10\}$ denoting the pulse number in one period of the mechanical motion. With $k \leqslant 4$, the QFI F increases very quickly at the initial pulse number n and arrives at a large constant value in the large-n limit. However, with the increase in $k \geqslant 5$, the QFI F shows the behaviors of initially increasing with n and then gradually going down to 0 with large n. In this case, the value of the QFI is very small compared to that of $k \leqslant 4$. When the pulse period does not match the mechanical period, e.g., $k \equiv \frac{T_0}{\tau}$ is an irrational number, we also find that the value of QFI F becomes much smaller compared to the case where the periods match. More importantly, it is shown in Fig. 2(a) that the QFI F with $k = 4$ is optimal, and the reason for this is discussed in Sec. III B.

The physics of these behaviors of the QFI F can be understood as follows. Note that the parameter to be estimated is the mechanical frequency ω_m. If the period of the driving

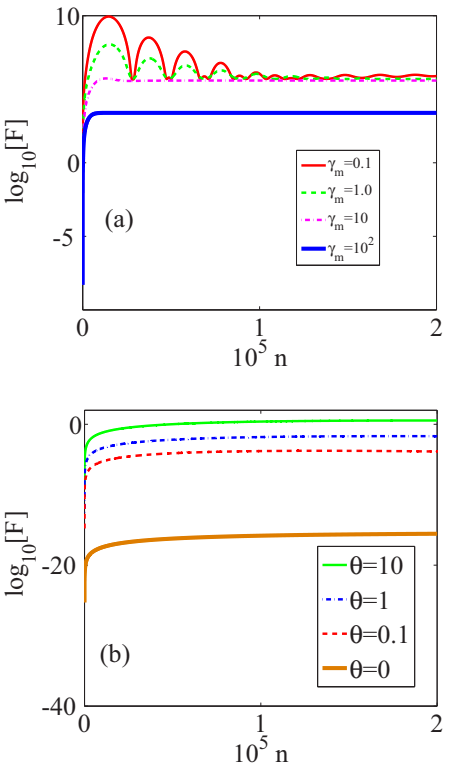

FIG. 3. The QFI F as a function of the pulse number n (a) at different decay rates γ_m (in Hz) for $\theta = 1.0$ and $k \equiv T_0/\tau = 1$ and (b) at different kick strengths θ for $\gamma_m = 10^2$ Hz and $\tau = 10^{-7}$ s. The other parameter is $n_{\rm th} = 100$. The QFI F is in units of Hz^{-2}.

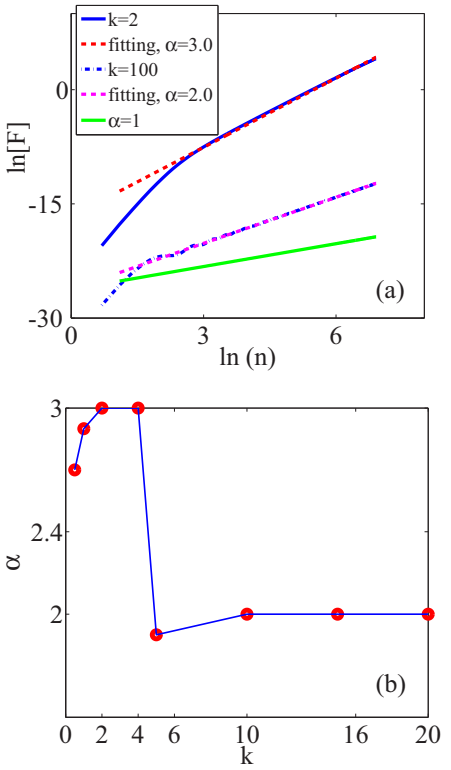

FIG. 4. (a) Fitting the increasing part of F with respect to the pulse number n. The index α is determined by numerically fitting $F \propto n^{\alpha}$. Both the x axis and the y axis are scaled based on the natural logarithm. The shot-noise limit ($\alpha = 1$) is displayed as the lowest (green) line. (b) The dependence of the index α on the parameter k. The other parameters are the same as in Fig. 2. The QFI F is in units of Hz^{-2}.

pulses τ matches that of the mechanical period T_0, the information of ω_m can be extracted to the greatest extent. As a result, the value of QFI F is large necessarily in the matching cases. A constant value of the QFI in the large n limit origins from the balance between the pulsed driving and the mechanical damping.

The influence of the mechanical decay rate γ_m on the QFI F is studied in the resonant driving regime, as shown in Fig. 3(a). This figure displays that with an increase in γ_m, the value of F decreases considerably. Moreover, F displays oscillation behavior when γ_m is very small. The reason for this oscillation is simple: the coherent evolution of the mechanical resonator, determined by ω_m, is dominated if the mechanics has a very high quantity factor $\frac{\omega_m}{\gamma_m}$.

The effect of the kick strength θ on the QFI F is shown in Fig. 3(b). It is obvious that F also decreases considerably with a decrease in θ. This can be easily understood: without external driving, the mechanical damping will suppress its coherence in the long-time limit. As a result, it is natural that the QFI F decreases.

In order to show the advantage of our pulsed driving estimation protocol, we illustrate in Fig. 4(a) the relationship between the increasing part of the QFI F and the pulse number n. We find that $F \propto n^{\alpha}$ by numerically fitting, with the index α dependent on the parameter k, as shown in Fig. 4(b). Moreover, we also checked numerically that this dependence of α on k is independent of the parameters γ_m and θ.

From Fig. 4(b), it is clear that the QFI F with respect to the pulse number n approaches the Heisenberg limit, with $\alpha = 2$ for the relatively large $k > 10$, similar to the results obtained previously in systems of a pulsed driving qubit [66,67]. For $k = 2, 4$, the QFI shows the behavior beyond the Heisenberg limit [68] with $\alpha = 3$. The Heisenberg limit and beyond displays that pulsed driving is an essential way to enhance the precision of parameter estimation.

In the following, we discuss how to read out the mechanical quadratures experimentally, which are required for the QFI of the mechanical resonator. For a pulsed optomechanical system, there exist at least two experimentally feasible schemes to achieve this aim. The main idea of the first one [51] is based on the homodyne detection of mixing between signal pulses, which interact with the mechanical resonator, and local oscillator pulses, as shown in Fig. 1(a) in Ref. [51]. The second scheme is based on the beam-splitter interaction, where mechanical quadratures are transferred into optical readout pulses (latter injected), as displayed in Fig. 2 in Ref. [49]. Thus, the information on the mechanical resonator can be gained from the output of the readout pulses.

IV. MECHANICAL SQUEEZING AS A QUANTUM RESOURCE

Generally, it is well known that the squeezed state [69], as an essential resource for quantum metrology [70,71], can enhance the precision of parameter estimation. Motivated by

this fact, we study the relationship between the QFI F and mechanical squeezing in this section.

Any single-mode Gaussian state can be expressed as [72]

$$\rho = \hat{D}(\alpha)\hat{S}(r,\phi)\rho_{\rm th}(\overline{n})\hat{S}^{\dagger}(r,\phi)\hat{D}^{\dagger}(\alpha), \tag{11}$$

where $\hat{D}(\alpha) = \exp[\alpha\hat{a} - \text{H.c.}]$ is the displacement operator of bosonic mode $\hat{a}$, $\hat{S}(r,\phi) = \exp[\frac{r}{2}(e^{-2i\phi}\hat{a}^2 - \text{H.c.})]$ is the squeezing operator, and $\rho_{\rm th}(\overline{m}) = \sum_{m=0}^{\infty} \frac{\overline{m}^2}{(\overline{m}+1)^{m+1}}|m\rangle\langle m|$ denotes the thermal state, with $\overline{m}$ the mean particle number. The squeezing strength r and the squeezing angle ϕ are determined by

$$r = \frac{1}{2}\text{arcsinh}\left[\frac{1}{2}\left(\frac{\gamma}{\det \mathbf{\Sigma}_{\varphi}}\right)^{\frac{1}{2}}\right], \tag{12}$$

$$2\phi = \begin{cases} -\arcsin\left(\frac{2\Sigma_{\varphi,12}}{\sqrt{\gamma}}\right) & \text{if} \quad \Sigma_{\varphi,11} < \Sigma_{\varphi,22}, \\ \pi + \arcsin\left(\frac{2\Sigma_{\varphi,12}}{\sqrt{\gamma}}\right) & \text{if} \quad \Sigma_{\varphi,11} > \Sigma_{\varphi,22}, \end{cases} \tag{13}$$

with $\gamma = (\Sigma_{\varphi,22} - \Sigma_{\varphi,11})^2 + (2\Sigma_{\varphi,12})^2$. Here $\Sigma_{\varphi,ij}$ $(i,j = 1,2)$ is the element of the covariant matrix $\mathbf{\Sigma}_{\varphi}$ as defined in Eq. (A6).

By rearranging the second-order moments given in Eq. (9) as the covariant matrix, the squeezing strength r and the squeezing angle ϕ are obtained according to Eqs. (12) and (13). Note that $\alpha = 0$ for the mechanical resonator studied in this paper. In Fig. 2(b), we plot the mechanical squeezing strength r as a function of the pulse number n for $k \leqslant 4$. By combining Figs. 2(b) and 2(a), it is apparent that both the mechanical squeezing and the QFI are enhanced with an increase in k. As a result, this squeezing as a quantum metrology resource strengthens the QFI F. Although Fig. 2(b) only shows the case $k \leqslant 4$, similar results were found for the other k values (not displayed here).

Based on the correlation between the QFI and the mechanical squeezing, we provide an intuitive way to understand the QFI for $k = 4$ (corresponding to a free rotation time $\tau = T_0/4$) being optimal with the kick strength $\theta = 1$. Toward this aim, it is useful to investigate the dynamics of the mechanical Wigner function, obtained according to Eq. (A8).

The kick operator $\mathbf{K}$ produces the mechanical squeezing, which remains invariant under free rotation $\mathbf{M}_0(\tau)$ (neglecting the mechanical damping). After the first kick acts on the mechanical resonator, the initial mechanical therm'al state translates into a squeezed state with squeezing angle $\phi(n = 1) \simeq \pi/8$, as shown in Fig. 5(a). Here ϕ is defined as the angle between the q axis and the direction of the squeezed quadrature. Then the squeezed state is rotated by $\vartheta = \omega_m T_0/4 = \pi/2$ along the clockwise direction by the free evolution $\mathbf{M}_0(\tau = T_0/4)$. Under the effect of the following kicks, the squeezing strength of the mechanical resonator progressively increases, as displayed in Figs. 5(b) and 5(c).

Moreover, the squeezing angle also gradually approaches $\phi \simeq \pi/4$ under some (e.g., $n \approx 10^2$) repetitive kicks (as well as the free evolution between kicks). Once the squeezing angle becomes $\phi = \pi/4$, which coincides with the counterpart angle produced by the squeezing action $\tilde{U}_{\theta=1} = \exp[-i(\hat{a}^2 + \text{H.c.})/2]$ in the kick operator $U_{\rm K}$, we find numerically that it will remain unchanged for the large-n limit. We would like to point out that here the matching between the squeezing angle

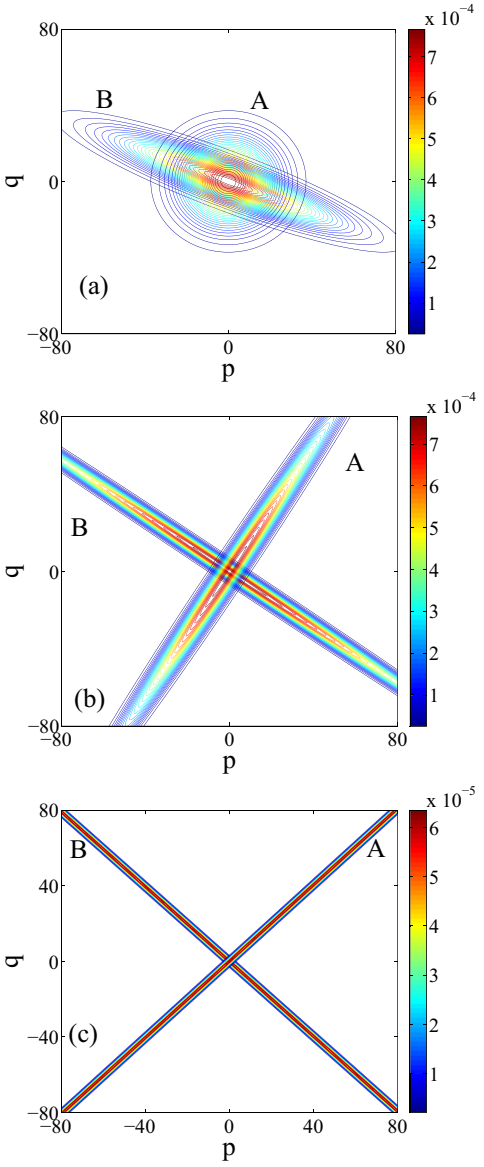

FIG. 5. The contours of Wigner functions of the mechanical resonator before (after) the nth kicked pulses are labeled A (B). The pulse number $n = 1$ (a), $n = 3$ (b), and $n = 10^3$ (c). It is obvious that here the mechanical squeezing can be strengthened by the kicks. The parameters are $k = 4$, $n_{\rm th} = 100$, and $\theta = 1.0$.

by kick and the free rotation angle plays an essential role in strengthening the mechanical squeezing. As a consequence, the QFI of the mechanical resonator is also enhanced.

We also show the mechanical Wigner function for the case $k = 5$ in Fig. 6, which corresponds to a free rotation angle $\vartheta = \omega_m T_0/5 = 2\pi/5$. Thus, after the free rotation (and considering the mechanical damping) represented by the operator $\mathbf{M}_0(\tau = T_0/5)$, the mechanical resonator cannot evolve into the squeezed state with the squeezing angle $\phi = \pi/4$ by the kick operator $U_{\rm K}$ in the long-time limit. This enables the kicks to squeeze the mechanical resonator ineffectively, as displayed in Fig. 6(c).

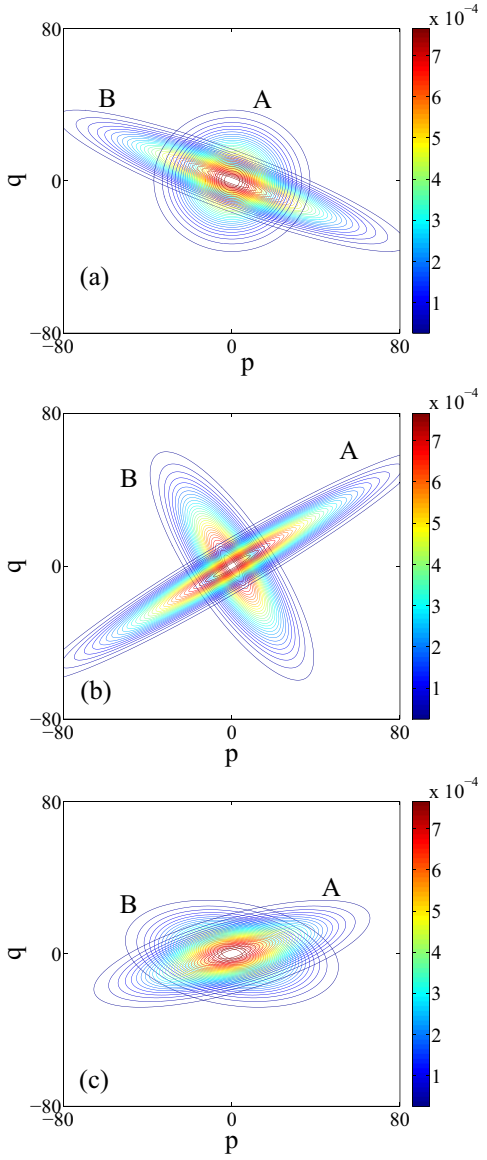

FIG. 6. The same as Fig. 5 except for the parameter $k = 5$, corresponding to the free rotation angle $\vartheta = 2\pi/5$. In this case, the kicks cannot effectively produce mechanical squeezing.

V. CONCLUSION

In summary, the quantum pulsed optomechanical system is proposed for application to the quantum metrology in the context of quantum parameter estimation by focusing on investigating the QFI. We find that the mechanical frequency can be estimated with a very high precision if the mechanical period matches that of the driving pulses. We also demonstrate that the mechanical squeezing is the quantum resource used in optimal quantum estimation of the frequency. In the future, it will be interesting to utilize coherence of the multimode cavity optomechanics [73,74] to enhance the accuracy of quantum parameter estimation.

ACKNOWLEDGMENTS

We thank X. G. Wang, X. W. Xu, H. Fu, and X. Xiao for their helpful discussions. This work was supported by the National Natural Science Foundation of China (Grants No. 11365006, No.11422437, No. 11121403, and No. 11565010), the 973 program (Grants No. 2012CB922104 and No. 2014CB921403), and the Guizhou Province Science and Technology Innovation Talent Team (Grant No. (2015)4015).

APPENDIX: QFI OF A SINGLE-MODE GAUSSIAN STATE

In order to be complete in this paper, here we review the main aspects of local quantum estimation theory, especially focusing on the QFI of a single-mode Gaussian state. Note that the mechanical resonator studied in this paper stays in a single-mode Gaussian state.

Let φ denote a single parameter to be estimated and $p(\zeta|\varphi)$ be the probability density with measurement outcome $\{\zeta\}$ for a continuous observable W conditioned on the fixed parameter φ. The value of the parameter φ can be inferred from the estimator function $\hat{\varphi} = \hat{\varphi}(\zeta_1, \ldots, \zeta_N)$, based on the measurement results $\zeta_1, \ldots, \zeta_N$ of N replicas of the system. Usually, this is achieved by the maximum likelihood estimation. With the definition of the classical Fisher information [75]

$$H_\varphi = \int d\zeta p(\zeta|\varphi)\left[\frac{\partial}{\partial\varphi}\ln p(\zeta|\varphi)\right]^2, \tag{A1}$$

the classical Cramér-Rao inequality [76] gives the bound of the variance $\mathrm{Var}(\hat{\varphi})$ for an unbiased estimator $\hat{\varphi}$:

$$\mathrm{Var}(\hat{\varphi}) \geqslant \frac{1}{H_\varphi}, \tag{A2}$$

Extending from the classical to the quantum regime, the conditional probability $p(\zeta|\varphi)$ is determined by the positive-operator-valued measure operator $\{\hat{E}_\zeta\}$ for a parameterized quantum state ρ_φ, $p(\zeta|\varphi) = \mathrm{Tr}[\hat{E}_\zeta\rho_\varphi]$. To determine the ultimate bound on precision posed by quantum mechanics, the Fisher information must be maximized over all possible measurements [77].

By introducing the symmetric logarithmic derivative L_φ determined by

$$\frac{\partial\rho_\varphi}{\partial\varphi} = \frac{1}{2}(\rho_\varphi L_\varphi + L_\varphi\rho_\varphi),$$

the so-called quantum Cramér-Rao inequality gives a bound on the variance of any unbiased estimator [78],

$$\mathrm{Var}(\hat{\varphi}) \geqslant \frac{1}{H_\varphi} \geqslant \frac{1}{F_\varphi}, \tag{A3}$$

where

$$F_\varphi = \mathrm{Tr}\left[\rho_\varphi L_\varphi^2\right] \tag{A4}$$

is the QFI.

The two bounds on the precision of parameter estimation [79] have been found, the so-called shot-noise limit $1/\sqrt{N}$ and the Heisenberg limit $1/N$. Usually, here N is the total particle number contributed to quantum estimation.

It is not easy to give the explicit formula of the QFI for a general system. Fortunately, the QFI is related to the Bures distance [78] through

$$D_B^2[\rho_\varphi, \rho_{\varphi+d\varphi}] = \frac{1}{4}F_\varphi d\varphi^2, \tag{A5}$$

where the definition of the Bures distance between two quantum states, ρ and σ, is [80]

$$D_B[\rho,\sigma] = [2(1 - \mathrm{Tr}\sqrt{\rho^{1/2}\sigma\rho^{1/2}})]^{1/2}.$$

The Wigner function for an arbitrary given state ρ, defined as

$$W(q,p) = \frac{1}{2\pi}\int_{-\infty}^{\infty} ds e^{-ips}\langle q - s|\rho|q + s\rangle,$$

can be used to equivalently represent the corresponding quantum state ρ, as there is a one-to-one correspondence between them. The Gaussian state, as a specific kind of continuous-variable state, has wide applications in actual quantum information processing [81]. They can be reproduced efficiently and unconditionally in the experiment. The unconditionedness is one advantage of the continuous-variable state, which is hard to achieve with a qubit-based discrete variable.

A state is said to be Gaussian when its Wigner function is Gaussian. A Gaussian state can be completely characterized by the first-order moment and the second-order moment:

$$\begin{aligned}\overline{X_i} &= \langle \hat{X}_i\rangle,\\ \Sigma_{\varphi,ij} &= \frac{1}{2}\langle(\hat{X}_i\hat{X}_j + \hat{X}_j\hat{X}_i)\rangle - \langle\hat{X}_i\rangle\langle\hat{X}_j\rangle\\ &= \int W(\vec{X})X_iX_jd^2\vec{X}.\end{aligned} \tag{A6}$$

Here

$$\vec{\hat{X}} \equiv (\hat{q},\hat{p}), \quad \langle\cdots\rangle \equiv \mathrm{Tr}(\rho_\varphi\ldots), \tag{A7}$$

and φ is the parameter to be estimated in the quantum state ρ_φ. The Wigner function is related to the second-order moments as (setting the first-order moments to 0)

$$W(\vec{X}) = \frac{1}{2\pi\sqrt{\mathrm{Det}\boldsymbol{\Sigma}_\varphi}}\exp\left(-\frac{1}{2}\vec{X}\boldsymbol{\Sigma}_\varphi{}^{-1}\vec{X}^T\right). \tag{A8}$$

Based on the fidelity between the arbitrary single-mode Gaussian states ρ_1 and ρ_2,

$$f(\rho_1,\rho_2) = \frac{2\exp\left[-\frac{1}{2}\Delta X^T(\boldsymbol{\Sigma}_1+\boldsymbol{\Sigma}_2)^{-1}\Delta X\right]}{\sqrt{|\boldsymbol{\Sigma}_1+\boldsymbol{\Sigma}_2| + (1-|\boldsymbol{\Sigma}_1|)(1-|\boldsymbol{\Sigma}_2|)} - \sqrt{(1-|\boldsymbol{\Sigma}_1|)(1-|\boldsymbol{\Sigma}_2|)}}, \tag{A9}$$

and making use of Eq. (A5), the QFI of the single-mode Gaussian state is found to be [82,83]

$$F_\varphi = \frac{\mathrm{Tr}\left[\boldsymbol{\Sigma}_\varphi^{-1}\boldsymbol{\Sigma}_\varphi'^2\right]}{2\left(1+P_\varphi^2\right)} + 2\frac{P_\varphi'^2}{1-P_\varphi^4} + \Delta\vec{X}_\varphi'^T\boldsymbol{\Sigma}_\varphi^{-1}\Delta\vec{X}_\varphi'. \tag{A10}$$

Here $\Delta\vec{X} = \langle\vec{X}_1 - \vec{X}_2\rangle$ is the mean relative displacement, $P_\varphi = |\boldsymbol{\Sigma}_\varphi|^{-1/2}$ denotes the purity of the state, and

$$\Delta\vec{X}_\varphi' = d\langle\vec{X}_{\varphi+\epsilon} - \vec{X}_\varphi\rangle/d\epsilon|_{\epsilon=0}. \tag{A11}$$

We note that the quantum Cramér-Rao bound of two-mode Gaussian states [84] was investigated previously.

[1] V. Giovannetti, S. Lloyd, and L. Maccone, Science **306**, 1330 (2004); Phys. Rev. Lett. **96**, 010401 (2006); Nat. Photon. **5**, 222 (2011).

[2] L. Pezzé and A. Smerzi, Phys. Rev. Lett. **102**, 100401 (2009); A. Smerzi, *ibid.* **109**, 150410 (2012).

[3] X. M. Lu, X. G. Wang, and C. P. Sun, Phys. Rev. A **82**, 042103 (2010); W. Zhong, Z. Sun, J. Ma, X. G. Wang, and F. Nori, *ibid.* **87**, 022337 (2013).

[4] Y. Yao, L. Ge, X. Xiao, X. G. Wang, and C. P. Sun, Phys. Rev. A **90**, 022327 (2014).

[5] Y. M. Zhang, X. W. Li, W. Yang, and G. R. Jin, Phys. Rev. A **88**, 043832 (2013).

[6] Q. Zheng, L. Ge, Y. Yao, and Q. J. Zhi, Phys. Rev. A **91**, 033805 (2015).

[7] T. Nagata, R. Okamoto, J. L. OBrien, K. Sasaki, and S. Takeuchi, Science **316**, 726 (2007).

[8] I. Afek, O. Ambar, and Y. Silberberg, Science **328**, 879 (2010).

[9] F. Hudelist, J. Kong, C. Liu, J. Jing, Z. Y. Ou, and W. P. Zhang, Nat. Commun. **5**, 3049 (2014).

[10] H. Strobel, W. Muessel, D. Linnemann, T. Zibold, D. B. Hume, L. Pezzè, A. Smerzi, and M. K. Oberthaler, Science **345**, 424 (2014).

[11] W. D. Li, T. C. He, and A. Smerzi, Phys. Rev. Lett. **113**, 023003 (2014).

[12] G. Q. Liu, Y. R. Zhang, Y. C. Chang, J. D. Yue, H. Fan, and X. Y. Pan, Nat. Commun. **6**, 6726 (2015).

[13] N. Zhao and Z. Q. Yin, Phys. Rev. A **90**, 042118 (2014).

[14] K. Iwasawa, K. Makino, H. Yonezawa, M. Tsang, A. Davidovic, E. Huntington, and A. Furusawa, Phys. Rev. Lett. **111**, 163602 (2013).

[15] S. Z. Ang, G. I. Harris, W. P. Bowen, and M. Tsang, New. J. Phys. **15**, 103028 (2013).

[16] M. Tsang, New. J. Phys. **15**, 073005 (2013).

[17] T. J. Kippenberg and K. J. Vahala, Science **321**, 1172 (2008).

[18] M. Aspelmeyer, P. Meystre, and K. C. Schwab, Phys. Today **65**, 29 (2012); P. Meystre, Ann. Phys. (Berlin) **525**, 215 (2013).

[19] M. Aspelmeyer, T. J. Kippenberg, and F. Marquardt, *Cavity Optomechanics* (Springer-Verlag, Berlin, 2014).

[20] M. Aspelmeyer, T. J. Kippenberg, and F. Marquardt, Rev. Mod. Phys. **86**, 1391 (2014).

[21] L. F. Buchmann, L. Zhang, A. Chiruvelli, and P. Meystre, Phys. Rev. Lett. **108**, 210403 (2012); H. T. Tan, F. Bariani, G. X. Li, and P. Meystre, Phys. Rev. A **88**, 023817 (2013).

[22] W. Marshall, C. Simon, R. Penrose, and D. Bouwmeester, Phys. Rev. Lett. **91**, 130401 (2003).

[23] F. Xue, Y. X. Liu, C. P. Sun, and F. Nori, Phys. Rev. B **76**, 064305 (2007).

[24] D. Rugar, R. Budakian, H. J. Mamin, and B. W. Chui, Nature (London) **430**, 329 (2004); A. G. Krause, M. Winger, T. D. Blasius, Q. Lin, and O. Painter, Nat. Photon. **6**, 768 (2012).

[25] C. A. Regal, J. D. Teufel, and K. W. Lehnert, Nat. Phys. **4**, 555 (2008).

[26] J. D. Teufel, T. Donner, M. A. Castellanos-Beltran, J. W. Harlow, and K. W. Lehnert, Nat. Nanotechnol. **4**, 820 (2009).

[27] S. Forstner, S. Prams, J. Knittel, E. D. van Ooijen, J. D. Swaim, G. I. Harris, A. Szorkovszky, W. P. Bowen, and H. Rubinsztein-Dunlop, Phys. Rev. Lett. **108**, 120801 (2012).

[28] X. Xu and J. M. Taylor, Phys. Rev. A **90**, 043848 (2014).

[29] A. Arvanitaki and A. A. Geraci, Phys. Rev. Lett. **110**, 071105 (2013).

[30] S. Mancini, D. Vitali, and P. Tombesi, Phys. Rev. Lett. **90**, 137901 (2003).

[31] Sh. Barzanjeh, S. Guha, C. Weedbrook, D. Vitali, J. H. Shapiro, and S. Pirandola, Phys. Rev. Lett. **114**, 080503 (2015).

[32] S. Weis, R. Rivière, S. Deléglise, E. Gavartin, O. Arcizet, A. Schliesser, and T. J. Kippenberg, Science **330**, 1520 (2010); A. H. Safavi-Naeini, T. P. M. Alegre, J. Chan, M. Eichenfield, M. Winger, Q. Lin, J. T. Hill, D. E. Chang, and O. Painter, Nature (London) **472**, 69 (2011).

[33] G. S. Agarwal and S. Huang, Phys. Rev. A **81**, 041803(R) (2010).

[34] I. Wilson-Rae, N. Nooshi, W. Zwerger, and T. J. Kippenberg, Phys. Rev. Lett. **99**, 093901 (2007); F. Marquardt, J. P. Chen, A. A. Clerk, and S. M. Girvin, *ibid.* **99**, 093902 (2007).

[35] C. Genes, D. Vitali, P. Tombesi, S. Gigan, and M. Aspelmeyer, Phys. Rev. A **77**, 033804 (2008).

[36] J. D. Teufel, T. Donner, D. Li, J. H. Harlow, M. S. Allman, K. Cicak, A. J. Sirois, J. D. Whittaker, K. W. Lehnert, and R. W. Simmonds, Nature (London) **475**, 359 (2011).

[37] Y. J. Guo, K. Li, W. J. Nie, and Y. Li, Phys. Rev. A **90**, 053841 (2014).

[38] J. Chan, T. P. Mayer Alegre, A. H. Safavi-Naeini, J. T. Hill, A. Krause, S. Groblacher, M. Aspelmeyer, and O. Painter, Nature **478**, 89 (2011).

[39] M. Paternostro, D. Vitali, S. Gigan, M. S. Kim, C. Brukner, J. Eisert, and M. Aspelmeyer, Phys. Rev. Lett. **99**, 250401 (2007); Sh. Barzanjeh, M. Abdi, G. J. Milburn, P. Tombesi, and D. Vitali, *ibid.* **109**, 130503 (2012).

[40] L. Tian, Phys. Rev. Lett. **110**, 233602 (2013); Y. D. Wang and A. A. Clerk, *ibid.* **110**, 253601 (2013).

[41] W. Wieczorek, S. G. Hofer, J. Hoelscher-Obermaier, R. Riedinger, K. Hammerer, and M. Aspelmeyer, Phys. Rev. Lett. **114**, 223601 (2015).

[42] M. R. Vanner, I. Pikovski, G. D. Cole, M. S. Kim, Č. Bruknera, K. Hammerer, G. J. Milburn, and M. Aspelmeyer, Proc. Natl. Acad. Sci. USA **108**, 16182 (2011).

[43] L. Viola and S. Lloyd, Phys. Rev. A **58**, 2733 (1998).

[44] K. Hammerer, E. S. Polzik, and J. I. Cirac, Phys. Rev. A **72**, 052313 (2005).

[45] O. Romero-Isart, A. C. Pflanzer, M. L. Juan, R. Quidant, N. Kiesel, M. Aspelmeyer, and J. I. Cirac, Phys. Rev. A **83**, 013803 (2011).

[46] M. Asjad, G. S. Agarwal, M. S. Kim, P. Tombesi, G. Di Giuseppe, and D. Vitali, Phys. Rev. A **89**, 023849 (2014).

[47] J. Q. Liao and C. K. Law, Phys. Rev. A **84**, 053838 (2011).

[48] S. G. Hofer, W. Wieczorek, M. Aspelmeyer, and K. Hammerer, Phys. Rev. A **84**, 052327 (2011).

[49] T. A. Palomaki, J. D. Teufel, R. W. Simmonds, and K. W. Lehnert, Science **342**, 710 (2013).

[50] Q. Y. He and M. D. Reid, Phys. Rev. A **88**, 052121 (2013); S. Kiesewetter, Q. Y. He, P. D. Drummond, and M. D. Reid, *ibid.* **90**, 043805 (2014).

[51] M. R. Vanner, J. Hofer, G. D. Cole, and M. Aspelmeyer, Nat. Commun. **4**, 2295 (2013).

[52] S. Machnes, J. Cerrillo, M. Aspelmeyer, W. Wieczorek, M. B. Plenio, and A. Retzker, Phys. Rev. Lett. **108**, 153601 (2012).

[53] O. Arcizet, P. F. Cohadon, T. Briant, M. Pinard, and A. Heidmann, Nature (London) **444**, 71 (2006).

[54] G. Anetsberger, O. Arcizet, Q. P. Unterreithmeier, R. Rivière, A. Schliesser, E. M. Weig, J. P. Kotthaus, and T. J. Kippenberg, Nat. Phys. **5**, 909 (2009).

[55] N. Kiesel, F. Blaser, U. Delić, D. Grass, R. Kaltenbaek, and M. Aspelmeyer, Proc. Natl. Acad. Sci. USA **110**, 14180 (2013).

[56] T. P. Purdy, D. W. C. Brooks, T. Botter, N. Brahms, Z.-Y. Ma, and D. M. Stamper-Kurn, Phys. Rev. Lett. **105**, 133602 (2010).

[57] J. C. Sankey, C. Yang, B. M. Zwickl, A. M. Jayich, and J. G. E. Harris, Nat. Phys. **6**, 707 (2010).

[58] J. D. Thompson, B. M. Zwickl, A. M. Jayich, F. Marquardt, S. M. Girvin, and J. G. E. Harris, Nature (London) **452**, 72 (2008).

[59] Z. J. Deng, Y. Li, M. Gao, and C. W. Wu, Phys. Rev. A **85**, 025804 (2012).

[60] G. Heinrich, J. G. E. Harris, and F. Marquardt, Phys. Rev. A **81**, 011801 (2010); H. Z. Wu, G. Heinrich, and F. Marquardt, New J. Phys. **15**, 123022 (2013).

[61] T. K. Paraiso, M. Kalaee, L. Zang, H. Pfeifer, F. Marquardt, and O. Painter, Phys. Rev. X **5**, 041024 (2015).

[62] M. Bhattacharya and P. Meystre, Phys. Rev. Lett. **99**, 073601 (2007); M. Bhattacharya, H. Uys, and P. Meystre, Phys. Rev. A **77**, 033819 (2008).

[63] A. Nunnenkamp, K. Børkje, J. G. E. Harris, and S. M. Girvin, Phys. Rev. A **82**, 021806(R) (2010).

[64] J. J. Li and K. D. Zhu, Phys. Rep. **525**, 223 (2013).

[65] N. E. Flowers-Jacobs, S. W. Hoch, J. C. Sankey, A. Kashkanova, A. M. Jayich, C. Deutsch, J. Reichel, and J. G. E. Harris, Appl. Phys. Lett. **101**, 221109 (2012).

[66] Y. Watanabe, T. Sagawa, and M. Ueda, Phys. Rev. Lett. **104**, 020401 (2010).

[67] Q. S. Tan, Y. X. Huang, X. L. Yin, L. M. Kuang, and X. G. Wang, Phys. Rev. A **87**, 032102 (2013).

[68] S. Boixo, A. Datta, S. T. Flammia, A. Shaji, E. Bagan, and C. M. Caves, Phys. Rev. A **77**, 012317 (2008); Y. C. Liu, G. R. Jin, and L. You, *ibid.* **82**, 045601 (2010).

[69] J. Ma, X. G. Wang, C. P. Sun, and F. Nori, Phys. Rep. **509**, 89 (2011).

[70] C. M. Caves, Phys. Rev. D **23**, 1693 (1981); M. D. Lang and C. M. Caves, Phys. Rev. Lett. **111**, 173601 (2013).

[71] L. Pezzé and A. Smerzi, Phys. Rev. Lett. **110**, 163604 (2013).

[72] C. Weedbrook, S. Pirandola, R. Garcia-Patron, N. J. Cerf, T. C. Ralph, J. H. Shapiro, and S. Lloyd, Rev. Mod. Phys. **84**, 621 (2012).

[73] X. W. Xu, Y. J. Zhao, and Y. X. Liu, Phys. Rev. A **88**, 022325 (2013).

[74] F. Massel, S. U. Cho, J. M. Pirkkalainen, P. J. Hakonen, T. T. Heikkilä, and M. Sillanpää, Nat. Commun. **3**, 987 (2012).

[75] R. A. Fisher, Proc. Cambridge Philos. Soc. **22**, 700 (1925).

[76] A. S. Holevo, *Probabilistic and Statistical Aspects of Quantum Theory* (North-Holland, Amsterdam, 1982).
[77] M. G. A. Paris, Int. J. Quantum. Inform. **7**, 125 (2009).
[78] S. L. Braunstein and C. M. Caves, Phys. Rev. Lett. **72**, 3439 (1994).
[79] S. L. Braunstein, C. M. Caves, and G. J. Milburn, Ann. Phys. (N.Y.) **247**, 135 (1996).
[80] M. A. Nielsen and I. L. Chuang, *Quantum Computation and Quantum Information* (Cambridge University Press, Cambridge, UK, 2000).
[81] A. Ferraro, S. Olivares, and M. G. A. Paris, *Gaussian States in Quantum Information*, *Napoli Series on Physics and Astrophysics* (Bibliopolis, Napoli, 2005).
[82] O. Pinel, P. Jian, N. Treps, C. Fabre, and D. Braun, Phys. Rev. A **88**, 040102 (2013).
[83] D. Delgado de Souza, M. G. Genoni, and M. S. Kim, Phys. Rev. A **90**, 042119 (2014).
[84] M. G. Genoni, P. Giorda, and M. G. A. Paris, Phys. Rev. A **78**, 032303 (2008); X. X. Zhang, Y. X. Yang, and X. B. Wang, *ibid.* **88**, 013838 (2013).